Structural Diversity and Plasticity Associated with Nucleotides Targeting Orotidine Monophosphate Decarboxylase

Ewa Poduch,[†] Lianhu Wei,[†,‡] Emil F. Pai,[†,§,△] and Lakshmi P. Kotra*[,†,‡,⊥,#]

Center for Molecular Design and Preformulations, Toronto General Research Institute, Toronto General Hospital, Toronto, Ontario, M5G 2C4 Canada, Departments of Pharmaceutical Sciences and Chemistry, University of Toronto, Toronto, Canada, Division of Cancer Genomics and Proteomics, Ontario Cancer Institute, Princess Margaret Hospital, 610 University Avenue, Toronto, Ontario, M5G 2M9, Canada, Departments of Medical Biophysics, Biochemistry, and Molecular and Medical Genetics, 1 King's College Circle, Toronto, Ontario, M5S 1A8, Canada, McLaughlin Center for Molecular Medicine, University of Toronto, Toronto, Ontario, Canada, and Department of Chemistry and Biochemistry, The University of North Carolina at Greensboro, Greensboro, North Carolina 27412

Received August 2, 2007

Orotidine monophosphate decarboxylase (ODCase) generally accepts pyrimidine-based mononucleotides as ligands, but other nucleotides are also known to bind to this enzyme. We investigated the kinetic properties of eight common and endogenous nucleotides with ODCases from three species: *Methanobacterium thermoautotrophicum*, *Plasmodium falciparum*, and *Homo sapiens*. UMP and XMP exhibited higher affinities as compared to the other nucleotides tested. The product of ODCase catalyzed decarboxylation, UMP, displayed inhibition constants (K_i) of 330 μM against the *Mt* enzyme and of 210 and 220 μM against the *Pf* and *Hs* ODCases, respectively. The K_i values for XMP were 130 μM and 43 μM, respectively, for *Mt* and *Pf* ODCases. Interestingly, XMP's affinity for human ODCase ($K_i = 0.71$ μM) is comparable and even slightly better than that of the substrate OMP. Binding of various nucleotides and their structural features in the context of ODCase inhibition and inhibitor design are discussed.

Introduction

Orotidine monophosphate decarboxylase (ODCase[a], EC 4.1.1.23) catalyzes the final step in the de novo biosynthetic pathway leading to uridine 5′-monophosphate (UMP).[1,2] This enzyme is present in all species ranging from unicellular organisms such as *Archaea* and various parasites to higher vertebrates including humans. The only known exception is viruses, which depend on the host cell for their supply of nucleotides during the replication process. The most interesting aspect of ODCase is its ability to accelerate the rate of decarboxylation of orotidine 5′-monophosphate (OMP) to produce UMP by over 17 orders of magnitude without the help of any cofactors or metal ions. The half-time ($t_{1/2}$) for the turnover of the substrate, OMP by ODCase (*S. cerevisiae*) is 18 msec; for the uncatalyzed reaction reportedly the corresponding value is about 78 million years.[2]

ODCase has been a fascinating enzyme to biochemists for over two decades. The chemical mechanism underlying its enormous rate acceleration is still discussed. In addition, its unusual biochemical capacity to also perform a "pseudohydrolysis" reaction or yielding to a covalent reaction involving one of its catalytic residues have established the enzyme's appeal as an enigmatic biochemical machine.[3–5] Recent discoveries that various C6-substituted nucleoside inhibitors of ODCase exhibit potent antimalarial activities have added a strong potential as a target for drug design.[6]

Our interest in the potential plasticity of the ODCase active site toward various nucleotide ligands and their structural diversity was generated by the fact that two common nucleotides, cytidine 5′-monophosphate (CMP) and xanthosine 5′-monophoshpate (XMP) could be cocrystallized with ODCases from *Mt* and *Pyrococcus horikoshii* OT3 (*Ph*).[7,8] This is particularly interesting because although the enzyme has evolved to accept uracil-type nucleic bases, XMP with its purine nucleic base binds at the same general site albeit with differences in the nucleic base orientation. Miller and co-workers reported that XMP and oxypurinol ribosyl phosphate inhibit yeast ODCase with K_is of 0.4 μM and 0.05 μM, respectively, comparable to or better than the binding affinity of the substrate ($K_M = 0.7$ μM).[13] This raises an interesting question: what general nucleotides are acceptable ligands for ODCases from various sources, and their importance in inhibitor design strategies. It is also very intriguing that, based on the preliminary structural evidence, some purine and pyrimidine nucleotides could bind to the ODCase active site in multiple modes.

To comprehend the scope of this plasticity, we investigated the eight most common mononucleotides to characterize their kinetic interactions with ODCases from *Methanobacterium thermoautotrophicum*, *Plasmodium falciparum*, and man and rationalize the results using three-dimensional models. The most common purine mononucleotides are adenosine- (AMP) and guanine-5′-monophosphate (GMP), while the most frequently encountered pyrimidine mononucleotides are cytosine- (CMP), thymidine- (TMP), and uridine-5′-monophosphate (UMP; Figure 1). Other important nucleotides include xanthosine- and inosine-5′-monophosphate (XMP and IMP, respectively), both intermediates in the biosynthesis of GMP, and are encountered during the metabolism of adenosine nucleotides. These findings

* To whom correspondence should be addressed. Mailing address: #5-356, Toronto Medical Discoveries Tower/MaRS Center, 101 College Street, Toronto, Ontario, M5G 1L7 Canada. Tel.: (416) 581-7601. Fax: (416) 581-7621. E-mail: lkotra@uhnres.utoronto.ca.

† Center for Molecular Design and Preformulations, Toronto General Research Institute.

‡ Departments of Pharmaceutical Sciences and Chemistry, University of Toronto.

§ Ontario Cancer Institute.

△ Departments of Medical Biophysics, Biochemistry, and Molecular and Medical Genetics, 1 King's College Circle.

⊥ McLaughlin Center for Molecular Medicine, University of Toronto.

The University of North Carolina at Greensboro.

[a] Abbreviations: ODCase, orotidine 5′-monophosphate decarboxylase; ITC, isothermal titration calorimetry; OMP, orotidine 5′-monophosphate.

10.1021/jm700968x CCC: $40.75
Published on Web 01/09/2008

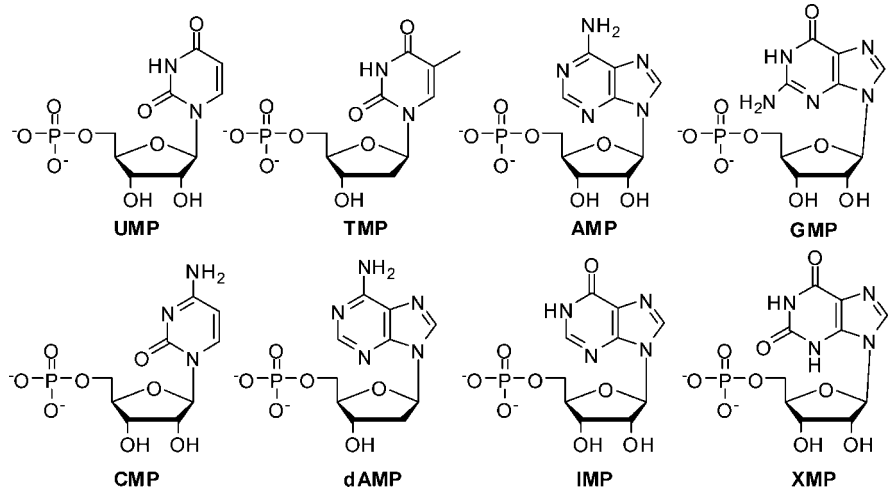

Figure 1. Chemical structures of purine and pyrimidine nucleotides.

may support efforts aimed at the design of novel nucleoside-based ODCase inhibitors carrying nucleic bases other than pyrimidines.

Materials and Methods

Enzymology. CMP disodium salt, TMP disodium salt, AMP disodium salt, dAMP disodium salt, XMP disodium salt, GMP disodium salt hydrate, IMP disodium salt, UMP disodium salt, and OMP trisodium salt were purchased from Sigma (Oakville, Ontario, Canada). Enzymatic assays were performed at 37 °C (*Pf* and *Hs*) or 55 °C (*Mt*) on the isothermal titration calorimeter (VP-ITC, MicroCal, MA), as described earlier.[5] ODCases from *Mt* and *Pf* were cloned, expressed, and purified, as described previously.[6,9]

Subcloning, Expression, and Purification of Hs ODCase. In humans, the ODCase activity resides in the C-terminal domain of the bifunctional enzyme UMP-synthase. The gene sequence corresponding to amino acids 190–480 of the C-terminal domain, with codons optimized for *E. coli* expression, was synthesized and inserted between the *Nde1* and *BamH1* restriction sites of the pET15b vector, which contains a His_6-tag for ease of purification. For expression, the plasmid was transformed into the *E. coli* strain BL-21 (Gold). The bacteria were cultured in LB broth at 25 °C and protein expression was induced with 100 mg/L IPTG at OD_{600} of 3. After 52 h, cells were harvested by centrifugation. The cells were then lysed by lysozyme, 50 mg/L, and nucleic acids were removed by incubation with DNase1. After centrifugation at 15000 rpm for 30 min, the clear supernatant was loaded onto a Ni column and was eluted with an imidazole gradient. The eluate, in 50 mM Hepes, pH 7.5, 500 mM NaCl, 5% glycerol, was concentrated to 2 mL by ultrafiltration. After the addition of one IU of thrombin and $CaCl_2$ to 2.5 mM, the solution was transferred into a dialysis bag and dialyzed against 2.5 mm $CaCl_2$, 50 mM HEPES, pH 7.5, 500 mM NaCl, 5% glycerol at 4 °C overnight. In a second pass over the Ni column, undigested His_6-tag protein and the free tag were removed as ODCase was eluted. If needed, a gel filtration on Sepharose 200 was added to further purify the protein. The eluate was concentrated to the desired protein concentration, TCEP was added to 1 mM for protection against oxidation, then the protein was flash-frozen and stored at −70 °C. The average yield of human ODCase was about 0.5 mg/L bacterial culture.

***Pf* ODCase.** A stock solution of 60 μM *Pf* ODCase (MW 39850 Da) for each experiment was prepared in 50 mM Tris, pH 7.5, 20 mM DTT, 40 mM NaCl, and incubated overnight at room temperature. OMP was dissolved in 50 mM Tris, pH 7.5, to a final concentration of 5 mM. The concentrated nucleotide solutions were also prepared in the same buffer. The enzyme activity was determined at 37 °C after a single 3.4 μL injection of OMP (5 mM) into the enzyme solution contained in the ITC reaction cell (1.3 mL). The inhibition assays were performed using competitive inhibition methods. The enzyme and inhibitor assay mixtures were prepared using a degassed buffer containing 50 mM Tris, pH 7.4, and 1 mM DTT. The final concentration of *Pf* ODCase in the reaction mixture was 60 nM, while the nucleotide concentration was varied. The concentrations of each nucleotide were as follows: AMP, 0, 2.5, 5, 10, 20 mM; dAMP, 0, 10, 20 mM; CMP, 0, 10, 20 mM; GMP, 0, 1, 2.5, 5, 10 mM; IMP, 0, 5, 10, 15, 20 mM; TMP, 0, 2.5, 5, 10, 20 mM; UMP, 0, 0.25, 0.5, 1 mM; XMP, 0, 0.025, 0.05, 0.1, 0.15, 0.25 mM.

***Mt* ODCase.** A 20 μM stock solution of *Mt* ODCase (MW 27344 Da) was prepared in 50 mM Tris, pH 7.5, 20 mM DTT, and 40 mM NaCl and incubated overnight at room temperature to allow enzyme stabilization. The inhibition of *Mt* ODCase was studied at 55 °C after a single injection of 5 mM OMP, resulting in 40 μM final substrate concentration. The assay samples containing 20 nM enzyme and inhibitor at various fixed concentrations were prepared in 50 mM Tris, pH 7.5, and 1 mM DTT. The concentrations of AMP were 0, 2, 3, 5, 10, 20 mM; for dAMP, 0, 2, 10, 20 mM; for CMP, 0, 0.5, 2, 5, 10 mM; for GMP, 0, 1, 2.5, 6, 10, 15 mM; for IMP, 0, 2.5, 5, 10, 20 mM; for TMP, 0, 0.5, 2, 5, 10 mM; for UMP, 0, 0.1, 0.25, 0.5, 1, 2 mM; and for XMP, 0, 0.025, 0.05, 0.1, 0.25, 0.5 mM.

***Hs* ODCase.** A 60 μM stock solution of human ODCase (MW 31710 Da) was prepared in 50 mM Tris, pH 7.5, 20 mM DTT, and 40 mM NaCl. The sample was incubated overnight at 4 °C. The enzyme was mixed with each compound using a buffer containing 50 mM Tris, pH 7.5, and 1 mM DTT, and the solution was transferred to the ITC sample cell. The enzyme activity in the absence and presence of nucleotides was monitored at 37 °C. The reaction was initiated by a 5.7 μL injection of 5 mM OMP. The final substrate concentration was 20 μM. The assay concentrations of each nucleotide were as follow: AMP, 0, 2, 5, 10, 25 mM; dAMP, 0, 2, 5, 10, 20 mM; CMP, 0, 1, 2, 5, 10 mM, GMP, 0, 1, 5, 10, 20 mM; IMP, 0, 2, 5, 10, 15, 20 mM; TMP, 0, 5, 10, 15, 20 mM; UMP, 0, 0.1, 0.25, 0.5, 1, 2 mM; and XMP, 0, 0.0025, 0.005, 0.01, 0.015, 0.025 mM.

Kinetic Data Analyses. The raw data were analyzed using the Origin 7.0 program. The typical data set containing the raw and analyzed data is represented in Figure 2. The raw data from the ITC experiment at various concentrations of the inhibitor provided characteristic valleys, as shown in Figure 2A. As the concentration of the inhibitor was increasing, the depth of the valley decreased. First, during the processing, the data were adjusted for the time delay (16 s) and the baseline was adjusted using the "Baseline" function. These data can then be converted into typical rate versus [*S*] plots for further interpretation (Figure 2B). As an example, the data sets with GMP are provided (Figure 2A,B). For in-depth description of the data analyses, please refer to ref 5. All data sets without inhibitors were converted to Michaelis–Menten curves for

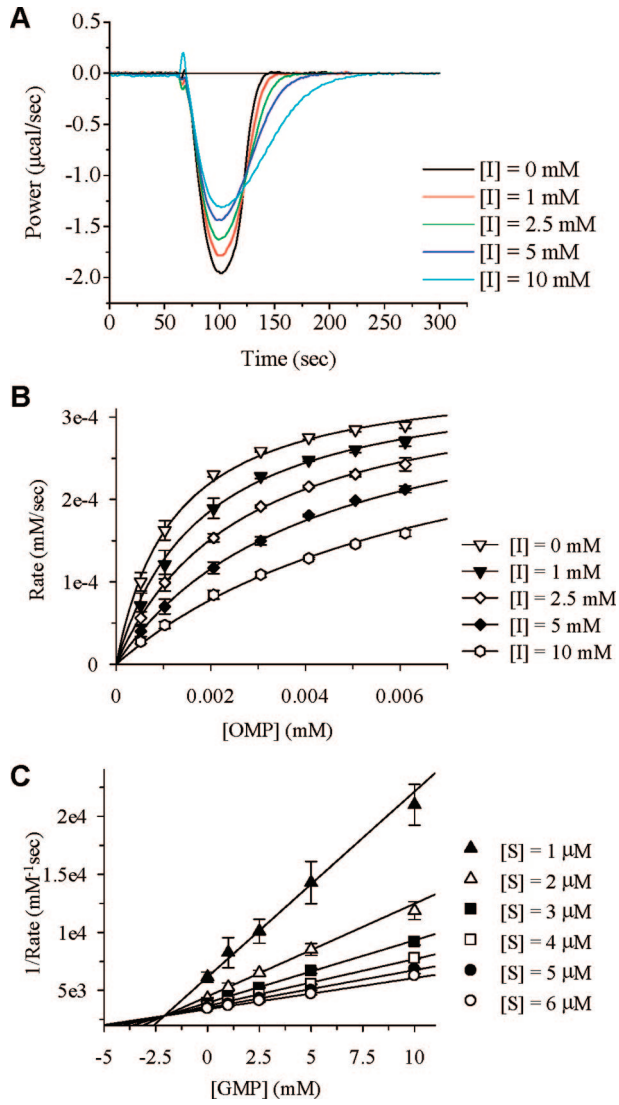

Figure 2. Inhibition of *Pf* ODCase by GMP. (A) Thermograms representing the reaction rate in the absence and presence of GMP. (B) The rate of decarboxylation of OMP in the absence and presence of GMP. (C) Dixon plot for the inhibition of ODCase by GMP.

Table 1. Kinetics Parameters for ODCases from Three Species *Mt*, *Pf*, and *Hs*

ODCase source	K_M (μM)	k_{cat} (s^{-1})
Mt	4.8 ± 0.9	20.7 ± 2.0
Pf	1.3 ± 0.1	6.7 ± 0.0
Hs	1.7 ± 0.3	8.1 ± 0.7

the measurement of kinetic parameters (specifically for the three ODCases) by fitting the data to eq 1

$$v = \frac{k_{cat}[E][S]}{K_M + [S]} \quad (1)$$

The data were then analyzed using the Grafit 5.0 data analysis package. Dixon plots were used to derive the inhibition patterns, and the inhibitors were competitive inhibitors (with an intersection point above *x*-axis). Where possible, the inhibition constant K_i was determined by fitting the rate versus [*S*] data to eq 2

$$v = \frac{k_{cat}[E][S]}{K_M\left(1 + \frac{[I]}{K_i}\right) + [S]} \quad (2)$$

The data from the above competitive experiments were also plotted using the double-reciprocal plots (1/rate vs 1/[OMP]) at various concentrations of each inhibitor to confirm that the inhibition is competitive in nature, and the K_i values are very similar from both methods. In Figure 7, double-reciprocal plots for XMP are presented. Please see Supporting Information for a comparison of the inhibition constants using Dixon plots and double-reciprocal plots for all the inhibitors (Tables S1 and S2, Supporting Information). When inhibition was not significant and only observable at rather high concentrations of the inhibitor the procedure described above could not be applied. A direct data fitting to eq 2 in Origin was performed to estimate the compound's dissociation constant. A weak inhibition was observed for dAMP with *Mt* ODCase using up to 20 mM of dAMP. Some compounds showed no inhibitory properties toward *Pf* and *Hs* ODCase.

Table 2. Inhibition Constants for Various Nucleotides against ODCases from *Mt*, *Pf*, and *Hs*[a]

	K_i (mM)		
ligand	*Mt*	*Pf*	*Hs*
AMP	3.5 ± 0.2	no inhibition	4.3 ± 0.2
dAMP	>10	no inhibition	7.4 ± 0.4
CMP	1.2 ± 0.7	no inhibition	1.4 ± 0.1
GMP	4.2 ± 0.1	2.1 ± 0.1	no inhibition
IMP	5.7 ± 0.2	4.0 ± 0.02	7.2 ± 0.3
TMP	3.3 ± 0.2	10.0 ± 0.6	8.7 ± 0.6
UMP	0.33 ± 0.01	0.21 ± 0.01	0.22 ± 0.1
XMP	0.13 ± 0.0034	0.043 ± 0.002	0.0007 ± 0.0003

[a] All inhibitors were evaluated in competitive assays against the ODCases. "No inhibition" indicates that the enzyme activity could not be inhibited using up to 10 or 20 mM of the inhibitor.

Structures of ODCase-Ligand Complexes. Three-dimensional structures of the inhibitors UMP, CMP, and XMP bound to *Mt* ODCase were obtained from the Research Collaboratory for Structural Bioinformatics (RCSB) PDB data bank (code: 1LOQ, 1LP6, and 1LOL, respectively). The complex of TMP bound to *Mt* ODCase was modeled from the corresponding complex with UMP (1LOQ) by mutating 5-H on uracil to a methyl group. Similarly, the complexes of ODCases with AMP and dAMP were built from the X-ray structure of the complex of XMP and *Ph* ODCase (2CZF). Structures of the complexes of UMP or CMP bound to *Pf* ODCase were generated from the crystal structure of the complex of 6-amino-UMP and *Pf* ODCase.[10] Computer modeling and structural analyses were performed using the Sybyl[11] software package running on an Octane2 IRIX operation system.

Results and Discussion

A series of eight common mononucleotides carrying various purine and pyrimidine nucleic bases are investigated to understand the diversity in the ligand structures for ODCase. These include UMP, TMP, CMP, AMP, dAMP, GMP, XMP, and IMP (Figure 1). While UMP is anticipated to bind with some affinity because it is the product of decarboxylation reaction catalyzed by ODCase, there were some interesting and surprising profiles of binding observed when ODCases from three different species were compared. In this context, ODCases from *P. falciparum* (*Pf*), *M. thermoautotrophicum* (*Mt*), and *H. sapiens* (*Hs*) are used to investigate the enzyme inhibition kinetics. For *Hs* ODCase, the bifunctional human UMP synthase is truncated, and the C-terminal portion carrying the ODCase activity is used in the experiments. Ligands were analyzed from two different perspectives: (i) all ligands were comprehensively evaluated for their inhibitory potential of all three ODCase activities, and (ii) structural information either from X-ray crystallography or from three-dimensional models was used to analyze various ligands' interactions within the active sites of ODCases. These analyses together provided a unique viewpoint of this interesting decarboxylase and its preferences for various ligands.

Previously, two mononucleotides UMP and XMP were kinetically and structurally characterized with respect to their

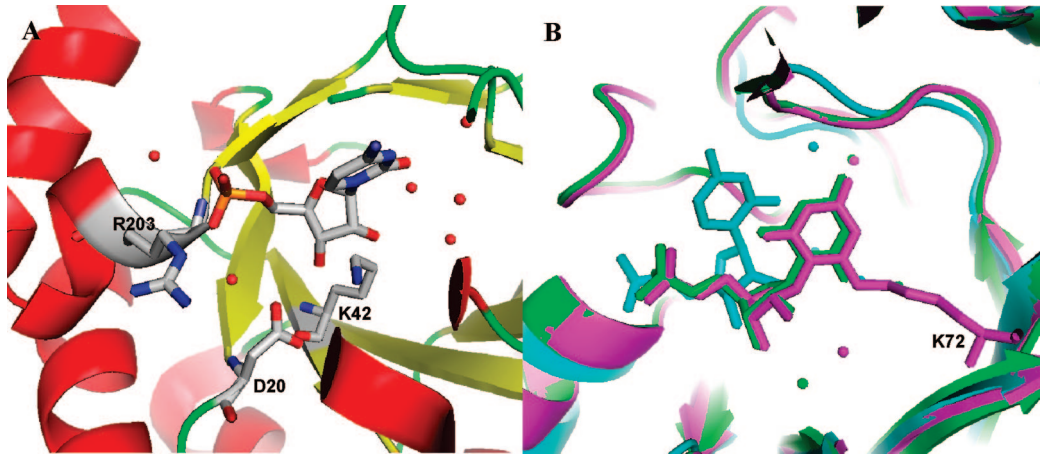

Figure 3. (A) X-ray structure of the complex of *Mt* ODCase with CMP (1LP6). CMP and the residues involved in hydrogen bonds with CMP are shown in capped stick model rendered according to atom type (red, O; white, C; blue, N; orange, P). (B) Overlap of the complexes of *Mt* ODCase with CMP, BMP, and 6-iodo-UMP. ODCase complexes with CMP, BMP, and 6-iodo-UMP (covalent bond with the uracil moiety) are presented in cyan, green, and magenta, respectively.

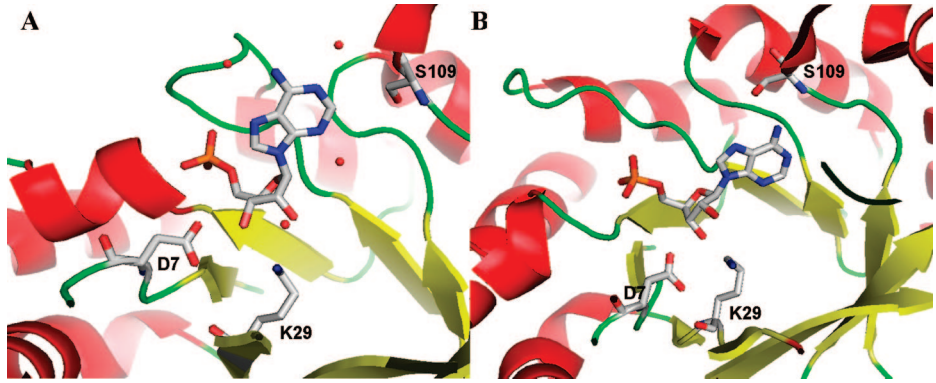

Figure 4. The model of the complex of *Ph* ODCase bound by AMP. The two bound conformations (panels A and B) are modeled after the two conformations seen for XMP in the catalytic site of *Ph* ODCase.

inhibitory activity toward ODCase from *S. cerevisiae*.[12,13] The competitive nature of UMP inhibition was confirmed by X-ray crystallography when this compound was cocrystallized with the *Mt* ODCase (PDB code: 1LOQ).[9] The XMP (1LOL) as well as CMP (1LP6) bind in the active site of *Mt* ODCase. Although the purine and pyrimidine bases did not form any hydrogen bonds with the active site residues, the electron density map clearly showed that both compounds occupy the active site, thereby preventing the substrate from binding.

Table 2 summarizes the inhibitory properties of various common purine and pyrimidine nucleotides against ODCases from *Mt*, *Pf*, and *Hs*. These three ODCases are quite different, by simply comparing their origin; *Mt* ODCase operates optimally at 55 °C and belongs to *Archea*; *Pf* ODCase is a monofunctional enzyme in a unicellular organism, and finally, *Hs* ODCase is a truncated C-terminal portion of the bifunctional human enzyme UMP synthase. The catalytic active sites of these three enzymes are identical, although there is significant difference in other portions of the protein sequence. Kinetic parameters (K_M and k_{cat}) for the enzymes from these three species *Mt*, *Pf*, and *Hs* provide a clue already that three enzymes operate with slightly different efficiencies (Table 1).

AMP, dAMP, and CMP, all three ligands carrying an amino moiety on their respective nucleic bases at C4 (for pyrimidine) or C6 (for purine) positions, were weak inhibitors of *Mt* and *Hs* ODCases, with low millimolar inhibition constants (Table 2). The trends in the inhibition constants (K_i) were similar for these two ODCases, although CMP is comparatively a stronger inhibitor with a K_i of 1.2 ± 0.7 and 1.4 ± 0.1 mM against *Mt* and *Hs* ODCases, respectively (Table 2). Interestingly, none of these compounds (AMP, dAMP and CMP) inhibited *Pf* ODCase up to 20 mM concentration. Earlier, Wu et al. cocrystallized CMP with *Mt* ODCase and showed that CMP binds with an unusual conformation in the binding site of ODCase, that is different from that of UMP and other uridine derivatives, such as the covalent inhibitor 6-iodo-UMP (Figure 3).[6,7] CMP, as observed in the X-ray crystal structure, is not in the best position to undergo optimal interactions in the active site, and this is evident through its inhibition kinetics as well. The phosphate group of CMP maintained a strong hydrogen bonding network with residues Arg203, Gly202, and two water molecules (Figure 3). The ribosyl moiety of CMP similarly exhibited hydrogen bonding interactions via 3′-hydroxyl moiety with Asp20 and Lys42, and via 2′-hydroxyl moiety with a water molecule. With just one hydrogen bond formed with a crystal water and the O2 oxygen, cytosine moiety of CMP does not contribute actively for binding, as gleaned from this three-dimensional structure of the complex.

The complexes of AMP and dAMP bound in the active site of ODCase were modeled by mutating the structure of XMP appropriately bound in the active site of *Ph* ODCase (Figure 4). Thus, we aligned the AMP with XMP in two different bound conformations seen for XMP in the binding site of *Ph* ODCase. *Ph* ODCase was chosen as the template because the crystal structure of the complex did not include a molecule of 1,3-butanediol bound in close proximity to the xanthine ring as

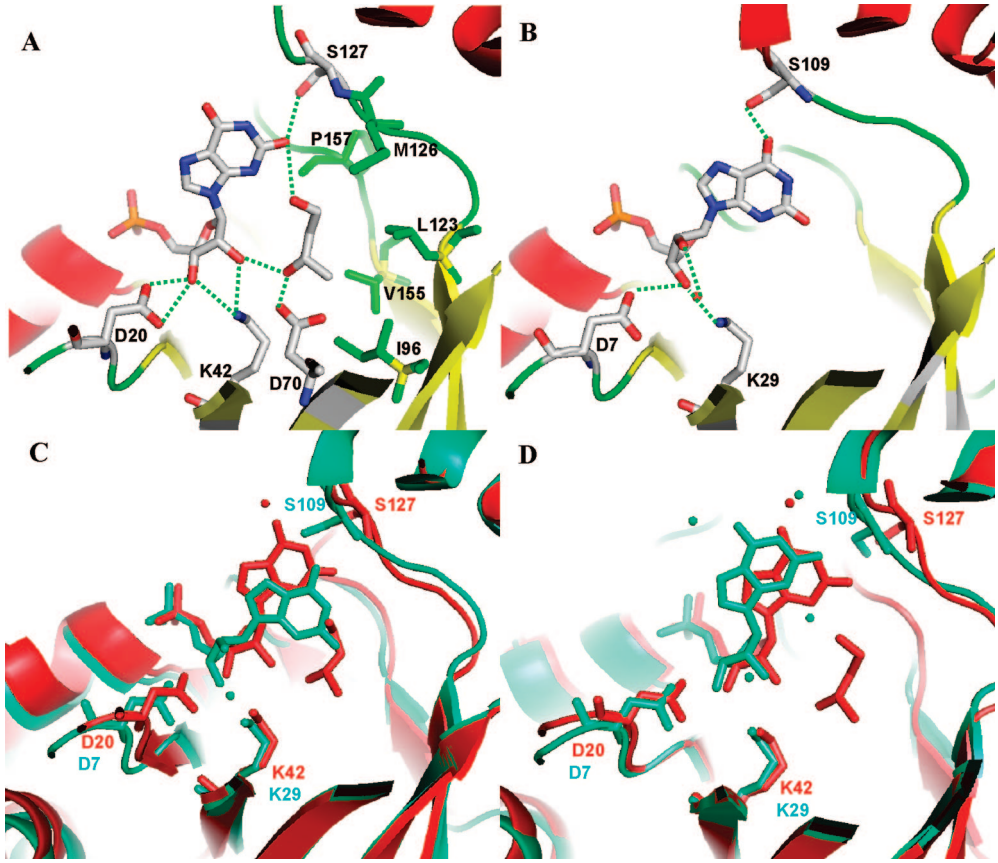

Figure 5. (A) The X-ray structure of the complex of XMP bound in the active site of *Mt* ODCase (1LOL). Residues contributed to binding site hydrophobic pocket are shown as a capped stick model in green. (B) XMP complexed with the ODCase from *Pyrococcus horikoshii* OT3 (2CZF). XMP structures are shown in capped stick representation (C, grey; O, red; N, blue; P, orange). Residues involved in hydrogen bonds with XMP are shown as a capped-stick model, and hydrogen bonds are depicted in broken lines in green. The hydrogen bonds are shown in broken lines in green. (C and D) Conformations of XMP bound in the active site of a monomer of the dimeric ODCase from *Pyrococcus horikoshii* OT3 (in cyan), in comparison to that from *Mt* (in red). XMP structures and the residues involved in hydrogen bonding formation are shown in a capped-stick representation.

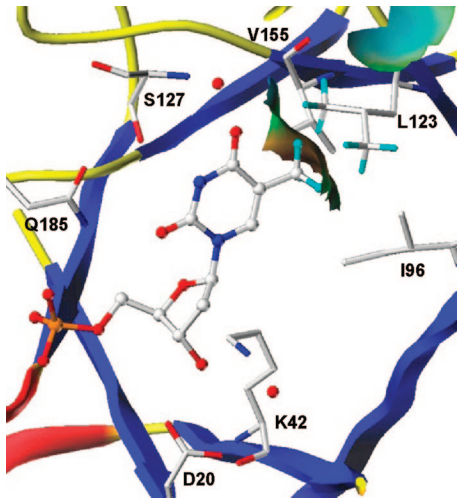

Figure 6. The model of the complex of TMP bound to ODCase.

reported for the *Mt* enzyme complex.[7] The only difference between AMP and dAMP bound models is that dAMP loses the interactions that are possible due to the hydroxyl moiety at 2′-position. This is reflected in the inhibition kinetics with AMP exhibiting 3.5 ± 0.2 mM inhibition constant against *Mt*, whereas the K_i for dAMP is 12 ± 0.3 mM, about 3–4-fold higher. A similar trend is also observed with *Hs* ODCase (Table 2). The adenine moiety in AMP (and in dAMP) is involved in three hydrogen bonds with either crystalline waters or Ser109, depending on its corresponding bound conformation (panels A vs B in Figure 4) in the active site of *Ph* ODCase.

GMP, with an amino moiety at the C2 position and a ketone at the C6 position on the purine base, exhibited very weak inhibition of ODCases from *Mt* and *Pf* (Figure 2) but did not inhibit that from *Hs* for up to 20 mM concentration of GMP. As seen from the Dixon plots, GMP is a competitive inhibitor of *Pf* ODCase (Figure 2C), with a K_i of 2.1 ± 0.1 mM. This is an interesting trend in comparison to that with AMP, which inhibited *Mt* and *Hs* ODCases but not *Pf* ODCase (vide supra). Analogous structures, IMP and XMP, behave interestingly, too. IMP, with a ketone moiety at the C6 of the purine ring, exhibited similar inhibition profiles against all three ODCases, and the K_i values are quite comparable to those with GMP. In addition, IMP did inhibit all three ODCases, unlike adenine and guanine mononucleotides.

A very interesting change in trend is that with XMP (Figure 7). Recently, XMP was cocrystallized with ODCases from *Mt* (PDB code: 1LOL) and *Pyrococcus horikoshii* OT3 (PDB code: 2CZF) by the Pai group and RIKEN Structural Genomics Initiative, respectively.[7,8] Miller et al. reported that XMP inhibits the yeast ODCase with a K_i of 0.4 μM.[13] The only difference between XMP and GMP is that there is a ketone moiety at the C2 position in XMP instead of an amino moiety. This structural change in the ligand considerably changes the corresponding inhibition profiles against ODCases. XMP inhibits *Mt* ODCase

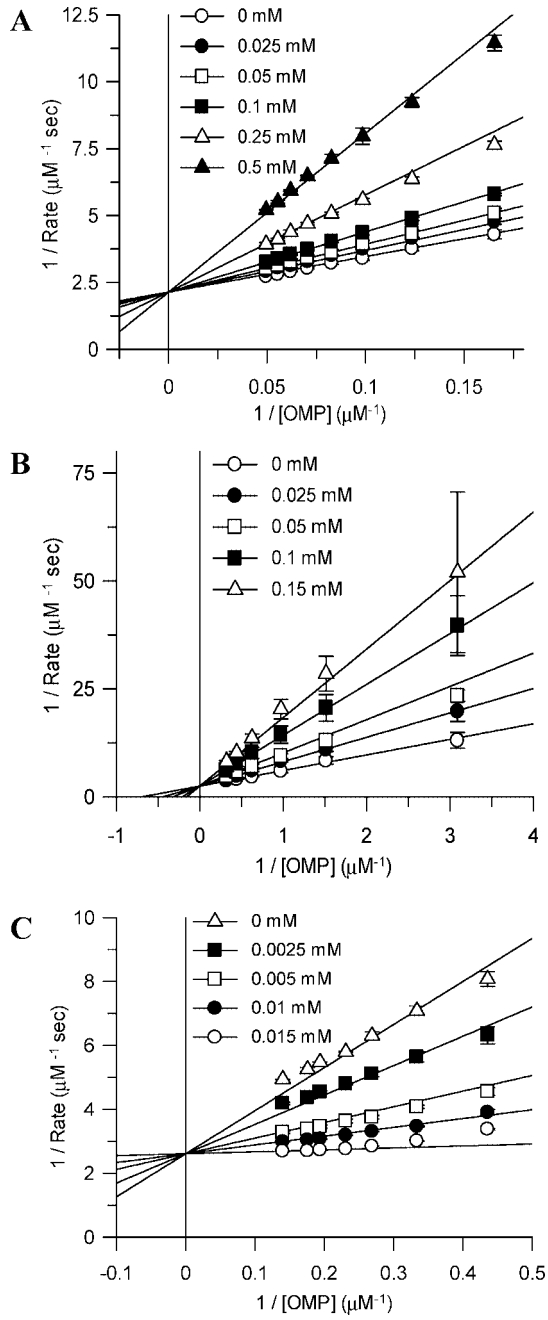

Figure 7. Double-reciprocal plots (1/rate vs 1/[OMP]) for the reversible inhibition of ODCases from *Mt* (A), *Pf* (B), and *Hs* (C) by XMP.

competitively with a K_i of 130 ± 3 μM (Figure 7). However, XMP inhibited *Pf* and *Hs* ODCases with almost 3-fold and 185-fold higher potencies competitively, with K_is 43 ± 2 and 0.71 ± 0.3 μM, respectively (Figure 7 and Table 2). The inhibition constant for *Hs* ODCase is similar to that against yeast ODCase. This is a remarkable potency for XMP, especially against *Hs* ODCase, which is within the range of the affinity of its own substrate (K_M for OMP, Table 1).

The three-dimensional structure of the complex of *Mt* ODCase and XMP shows a completely novel binding conformation for this nucleotide when compared to that of UMP (Figure 5).[7] First of all, the position of XMP in the binding site is away toward the opening of the binding site and outward than UMP, causing the residues Ile178−Phe195 shift outward from the binding pocket. Similar to UMP, however, the phosphate group of XMP maintains a good hydrogen bonding network with Arg203 or Arg294 (in *Mt* and *Ph* ODCases, respectively) and the four proximal crystalline waters. Other important interactions include the hydrogen bonding between 3′-hydroxyl moiety and the residues Asp20 and Lys42 and between the 2′-hydroxyl moiety and the crystalline water (Figure 5A). The xanthine group of XMP showed four hydrogen bonds with Ser127 and the crystalline waters, despite its shift in the binding site, thus allowing it to inhibit ODCase with moderate potency.

A comparison of the complex of XMP bound to *Ph* ODCase and that to *Mt* ODCase further revealed interesting interactions (Figure 5C,D). In the crystal structure with *Mt* ODCase, 1,3-butanediol is sandwiched between XMP and the side chains of Lys72 and Asp70 in the active site. The two hydroxyl groups on 1,3-butanediol formed hydrogen bonds with XMP, specifically with the 2′-hydroxyl moiety, O2 and N3 atoms on the purine. The hydrophobic region of the ligand fits in a hydrophobic pocket formed by the residues Ile96, Leu123, Met126, Val155, and Pro157 in the active site of ODCase. In the dimeric structure, the two XMP molecules were bound in a similar fashion one each in each monomer.

Interestingly, however, in the complex of XMP bound to *Ph* ODCase, the two XMP molecules bind in two different conformations in the two monomers of the dimer (ODCase always crystallizes as a dimeric unit). In the complex with *Ph* ODCase, there is no additional ligand other than XMP in the binding site. This permitted the binding of XMP halfway into the binding site, with an altered hydrogen bonding pattern between XMP and *Ph* ODCase (Figure 5A vs B). The carbohydrate conformation in *Mt* ODCase for XMP is 2′-exo/3′-endo, whereas that in *Ph* ODCase for XMP is 2′-endo/3′-exo, and such a change obviously shifts the orientation of the purine base dramatically (Figure 5C). Due to this change in the ribose conformation, the hydrogen bonding patterns for 2′- and 3′-hydroxyl moieties in *Mt* and *Ph* ODCases with XMP are quite different (broken lines in green in Figure 5A,B, respectively). In *Mt* ODCase, O2 in xanthine moiety is involved in two hydrogen bonds, with Ser127 and Pro157 (Figure 5A). But in the X-ray structure of *Ph* ODCase bound to XMP, O6 of the xanthine moiety (instead of O2 as in the case of *Mt* ODCase complex) interacts via one hydrogen bond only with Ser109 (Figure 5B).[8] More interestingly, the two XMP molecules in the dimeric unit exhibit variations in the binding conformation in the active site (Figure 5C,D). When these two conformations of XMP in the active site of *Ph* ODCase are compared to that in the active site of *Mt* ODCase, xanthine in one monomer of *Ph* ODCase showed very little overlap (Figure 5C), while that in the other monomer of *Ph* ODCase has somewhat similar orientation (Figure 5D). The various binding patterns of XMP in different species as well as in each monomer of the dimeric unit reveal the tolerance of this enzyme toward purine bases in different poses for binding.

The two pyrimidine nucleotides, TMP and UMP showed weak inhibitory potential of all three ODCases, as expected. TMP, carrying a 5-methyl group exhibited a K_i in the range of 3.3 ± 0.01 to 10.0 ± 0.6 mM (Table 2). An analysis of the model of the complex of TMP bound in the active site of *Mt* ODCase indicated that the 5-methyl group has potential steric crowding due to Leu123, creating an unfavorable environment for binding, despite potential strong interactions of the ribosyl moiety and the phosphate moiety (Figure 6). However, other regions of TMP interact similar to that observed with UMP, and UMP inhibits these ODCases with 5–10-fold higher potency that TMP. This is due to the fact that the steric crowding due to 5-methyl group is causing TMP to bind less favorably.

In general, UMP and TMP have very strong hydrogen bond networking interactions with ODCase. The phosphate group formed a total of nine hydrogen bonds with the surrounding residues Gln269, Arg294, and the four crystalline water molecules. The 2′-hydroxyl moiety of UMP interacts with Oγ1 of Thr79, and Oδ1 and Oδ2 of Asp75 via hydrogen bonding. The 3′-hydroxyl moiety similarly has several possibilities to engage in hydrogen bonds with the surrounding residues Lys42, Asp20, and a crystalline water molecule. Despite the three hydrogen bonds with the residues Ser127 and Gln185, the methyl group on C5 of the pyrimidine ring in TMP creates a crowded interaction with Leu123, compromising the inhibitory activity (Figure 6). This is reinforced by the fact that TMP does not possess a 2′-hydroxyl moiety, thus compromising the hydrogen bonding interactions of this moiety with the binding site. All together, this is costing TMP almost a 4–10-fold loss in potency in comparison to UMP against these ODCases. Inhibitory profiles against the three ODCases are very similar for these two pyrimidine derivatives (Table 1).

These data indicate that ODCases, as shown here from three different species, could accept interesting and diverse ligand structures for their binding in the active site. The inhibition potencies of these ligands could vary as much as 2 orders of magnitude, depending on the ODCase species of origin, but for the same inhibitor molecule. Their bound conformations could be different in the binding sites of ODCases. Interestingly, these differences underscore the "individuality" of each ligand toward the ODCase from each species. This is intriguing considering the fact that the active sites of ODCases are conserved across all species very tightly. Principles guiding this flexibility of nucleotide ligand structures and their conformations targeting ODCase activity should be explored further to completely understand this class of enzymes in addition to elucidating the catalytic mechanisms. The findings disclosed here will aid the design of novel and better nucleic bases other than the natural pyrimidines, as well as other diverse carbohydrate moieties.

Acknowledgment. The authors thank Dr. Hailun Tang and Ms. Wing Lau for their excellent help with the expression and purification of *Pf*, *Mt*, and *Hs* ODCase enzymes. We thank Dr. Raymond Hui for kindly providing the plasmid for *Pf* ODCase. We are grateful to Professor David Clarke, University of Toronto, for generously allowing the use of the VP-ITC instrument. This work was supported by grants from the Canadian Institutes of Health Research and the Canada Research Chairs program.

Supporting Information Available: Details of the thermograms and inhibition kinetic profiles with nucleotide ligands. This material is available free of charge via the Internet at http://pubs.acs.org.

References

(1) Miller, B. G.; Wolfenden, R. Catalytic proficiency: The unusual case of OMP decarboxylase. *Annu. Rev. Biochem.* **2002**, *71*, 847–885.
(2) Radzicka, A.; Wolfenden, R. A proficient enzyme. *Science* **1995**, *267*, 90–93.
(3) Bello, A. M.; Poduch, E.; Fujihashi, M.; Amani, M.; Li, Y.; Crandall, I.; Hui, R.; Lee, P. I.; Kain, K. C.; Pai, E. F.; Kotra, L. P. A potent, covalent inhibitor of orotidine 5′-monophosphate decarboxylase with antimalarial activity. *J. Med. Chem.* **2007**, *50*, 915–921.
(4) Fujihashi, M.; Bello, A. M.; Poduch, E.; Wei, L.; Annedi, S. C.; Pai, E. F.; Kotra, L. P. An unprecedented twist to ODCase catalytic activity. *J. Am. Chem. Soc.* **2005**, *127*, 15048–15050.
(5) Poduch, E.; Bello, A. M.; Tang, S.; Fujihashi, M.; Pai, E. F.; Kotra, L. P. Design of inhibitors of orotidine monophosphate decarboxylase using bioisosteric replacement and determination of inhibition kinetics. *J. Med. Chem.* **2006**, *49*, 4937–4945.
(6) Bello, A. M.; Poduch, E.; Liu, Y.; Wei, L.; Crandall, I.; Wang, X.; Dyanand, C.; Kain, K. C.; Pai, E. F.; Kotra, L. P. Structure–activity relationships of C6-uridine derivatives targeting plasmodia orotidine monophosphate decarboxylase. *J. Med. Chem.* **2008**, *51*, 439–448.
(7) Wu, N.; Pai, E. F. Crystal structures of inhibitor complexes reveal an alternate binding mode in orotidine-5′-monophosphate decarboxylase. *J. Biol. Chem.* **2002**, *277*, 28080–28087.
(8) Ito, K.; Arai, R.; Shirouzu, M.; Yokoyama, S. Crystal structure of orotidine 5′-phosphate decarboxylase from *Pyrococcus horikoshii* OT3 complexed with XMP. RIKEN Structural Genomics/Proteomics Initiative (RSGI). PDB ID: 2CZF, http://dx.doi.org/10.2210/pdb2czf/pdb.
(9) Wu, N.; Mo, Y.; Gao, J.; Pai, E. F. Electrostatic stress in catalysis: structure and mechanism of the enzyme orotidine monophosphate decarboxylase. *Proc. Natl. Acad. Sci. U.S.A.* **2000**, *97*, 2017–2022.
(10) PDB ID: 2Q8Z.pdb and ref 6.
(11) *SYBYL 7.0*, Tripos Inc., 1699 South Hanley Rd., St. Louis, MO, 63144.
(12) Miller, B. G.; Butterfoss, G. L.; Short, S. A.; Wolfenden, R. Role of enzyme-ribofuranosyl contacts in the ground state and transition state for orotidine 5′-phosphate decarboxylase: a role for substrate destabilization. *Biochemistry* **2001**, *40*, 6227–6232.
(13) Miller, B. G.; Snider, M. J.; Wolfenden, R.; Short, S. A. Dissecting a charged network at the active site of orotidine-5′-phosphate decarboxylase. *J. Biol. Chem.* **2001**, *276*, 15174–15176.

JM700968X